Research Paper

Optimization of 3D Steel Moment Frame Structures with Torsional Irregularity via PSO

Mahbobeh Mirzaie Aliabadi[1*], Milad Zargarshooshtari[2], Masoud Zargarshooshtari[3] and Mohammed Sadegh Shahidzade[1]

1. Assistant Professor, Department of Civil Engineering Faculty, Khatam Alanbia University of Technology, Behbahan, Iran, *Corresponding Author; email: mirzaie@bkatu.ac.ir
2. M.Sc., Department of Civil Engineering Faculty, Khatam Alanbia University of Technology, Behbahan, Iran
3. M.Sc., Department of Civil Engineering Faculty, Islamic Azad University, Ramhormoz, Iran

Received: 10/11/2022
Revised: 18/03/2023
Accepted: 19/03/2023

ABSTRACT

The aim of this study was to evaluate the optimization of three-dimensional steel moment frame structures with various irregularity in the plan, via particle swam algorithm under earthquake load. In this way, two types of three-dimensional steel moment frame structures have been modeled. The first structure has box-shaped columns assessed with 0 Percent, 20%, 40% and 60% load eccentricity. The second structure includes cross-shaped columns, which is evaluated with the same condition as the first structure. The particle swarm optimization (PSO) algorithm has been used to achieve the optimum structure considering weight, maximum drift, dimensional fit of joints and strong column-weak beam condition. In addition, in the optimizing process of elements, the required strength of the sections according to AISC360-10 is satisfied under the LRFD method. The AISC360-10 database is also used for sections of structures (I-shaped beams, box-shaped and cross-shaped columns). The results demonstrated that the proposed algorithm can design optimal structures with box shaped column which are only less than 12 percent heavier than a regular structure. For each %20 increase in the load eccentricity the weight of the optimal structure with box-shaped columns would increase by about %5. Moreover, the weight of the structure with the cross-shaped columns in the same noted condition was 0.31, 9.4 and 11.9% more than the weight of the structure in regular optimal state, respectively.

Keywords:
Steel structure; Box column; Cross column; Irregularity; Particle swarm optimization

1. Introduction

Structural engineers are concerned with designing efficient structures. However, achievement of such optimum designs is hindered by the complex structure of the design criteria. It is also important to prevail these challenges utilizing currently available computational power. Hence, researchers take note of meta-heuristic optimization algorithms as suitable tools for this purpose. Some of the common applied metaheuristic algorithms that are used for structural optimization are genetic algorithm (GA) [1], particle swarm optimization (PSO) [2], ant colony optimization (ACO) [3] and harmony search algorithm (HS) [4]. Among the noted algorithms, GA and PSO are some of the well-known techniques commonly used in optimization of steel moment frames [5].

The literature is indicative of the many researchers' attempts to minimize the weight of steel moment resisting frames by meta-heuristic algorithms considering elastic material behavior. An eagle strategy based on differential methods was used to find some suitable region and by this manner close results was obtained compared with mathematical approaches [6]. In another study, the big-bang big-crunch algorithm that is based on setting average weight on choices was used to optimize trusses and frames, in this attempt the weight of choices depends on the performance of the objective function [7]. Some investigators introduced an extended ant colony optimization (ACO) to improve the speed of the algorithm by decreasing the size of the trail matrix [8]. They also optimized structures by an imperialist competitive algorithm. This algorithm was based on countries and colonies. Agents were considered as countries which were organized in colonies. Agents of the corresponding colonies try to gather near the best one that is identified as empire [9]. In other field work, optimization of 3D steel space frames was presented by utilizing artificial bee colony algorithm with Levy flight distribution, while dimensional constraints and P-Δ analysis were considered [10]. Also, in another investigation, some researches optimized steel frames by the design-driven harmony search, in which the best results were observed in small number of iterations and this achievement was the goal of the work [11]. In another background check, an enhanced firefly algorithm was presented by Carbas to optimize 3D steel frame structures. The enhancement consisted changing algorithm parameters during design iteration to improve attractiveness and randomness properties of the algorithm [12].

There are also some studies that researchers applied various irregularities in steel moment frames to evaluate the effects on optimum structure's weight or measure the ability of optimization algorithm. For this purpose; Aydogdu and Saka [13] optimized irregular steel moment frames including elemental warping effect by ACO algorithm. The results showed that considering of warping increased weigh around %9 for regular and %12 for irregular frames of moderate size. In another work, the asymmetric genetic algorithm (AGA) was proposed by Eshaghi et al., to optimize 3D irregular and regular steel structures. The AGA was found to be advantageous regarding the time and number of analyses and successfully decreasing the weights of irregular and regular steel structures by %26.4 and %11.1, respectively [14]. Also, a comparison of four metaheuristic algorithms (CBO, ECBO, VPS and MDVC- UVPS) for optimization of 3D irregular steel structures revealed that the MDVC-UVPS resulted in the optimum solution in all featured cases [15].

The review of previous research showed that researchers paid less attention to optimization of structures with torsion irregularities [10, 12-14]. In most researches, an irregularity was considered by selecting an irregular plan. This has limited the previous studied to analyzing only a few structures. Noting that the effect of irregularity on the analysis can be modeled by addition of torsion to the lateral earthquake loads, by introducing specific distances between the center of mass and stiffness in model of structure, torsion can be applied without changing the geometry of the structures. Using this modeling technique, the effect of various irregularities was considered in this study using a regular plan (according to Regulation 2800 [16]), while the structure is optimized under the particle swarm optimization algorithm. Finally, the optimal weight of the structures under various irregularities was compared. Knowing this difference can be useful to design a lighter, more economical structure and is valuable for redesigning seismic frames.

Twisting of a building about vertical axis increases the shear force demand on lateral force resisting elements and it is not desirable as increased shear force results in brittle failure. Generally twisting is introduced in a building due to eccentricity between center of mass (CM) and center of stiffness (CS) at diaphragm level. Eccentricity can be induced in a structure due to mass, strength and stiffness arising out of various construction and design limitations. Codes insist to apply design forces calculated according to equivalent static method or response spectrum method at displaced center of mass so as to cause design eccentricity between CM and CS. The displaced center of mass resulting from design eccentricity consists of two terms; i.e., static eccentricity and accidental eccentricity. Also earthquake ground motion has the ability to introduce torsion in the structure. In the current work an adjustment of the mass eccentricity from 0 to 0.6 relative to plan dimension was considered while the center of rigidity was kept at the center of the plan [17].

In optimum design process, the LRFD design relations according to AISC-360-10 [18] was used and the weak beam and strong column seismic criteria was applied. Also, the particle swarm optimization was used to optimize structures. This paper is organized as follows: First, the optimization problem is defined and the variables, constraints and objective functions are described. Then the criteria for designing steel structural elements and moment frames are presented followed by explanation of the PSO algorithm. Finally, numerical examples and concluding remarks are presented.

2. Problem Definition

The main components of the present optimization problem are summarized in this section:

2.1. Objective Function

The objective function is the total weight of the structure and is expressed as Equation (1) :

$$W = \sum_{i=1}^{N} \rho_i l_i A_i \qquad (1)$$

where, N is the number of structure's members. ρ_i is the density of the steel; L_i is the length of i^{th} member; A_i is the section area of i^{th} member

2.2. Variables

The section area (A) of structure's member is variable of objective function to achieving the optimum weight. Determining this variable is based on the geometric dimensions of the members. In this study, three steel sections are considered to model the members. For beams, W sections are used. For columns, Hss and Chilipia sections (build from two W-shapes section) are considered. The best area of the members is defined in optimum process from geometric dimensions of sections as shown in Figure (1). All the sections are chosen from database of AISC 360-10 regulations.

2.3. Modeling Structural Irregularities

In this study, comparing optimum weight of steel moment frame structures, with various irregularities (0%, 20%, 40% and 60% [17]) are considered according to 2800 code [16]. For this purpose, the irregularity is considered by applying distance between center of mass and stiffness. In this manner, the center of stiffness is fixed in homolographic of plan by symmetric member grouping as shown in Figure (2), and the center of mass is displaced as shown in Figure (3). By this method, during the optimum process, the rate of eccentricity (rate of irregularity) does not change, and comparing the optimum weight of structures with considered irregularity can be achieved and the eccentricity will not change during the optimal design process.

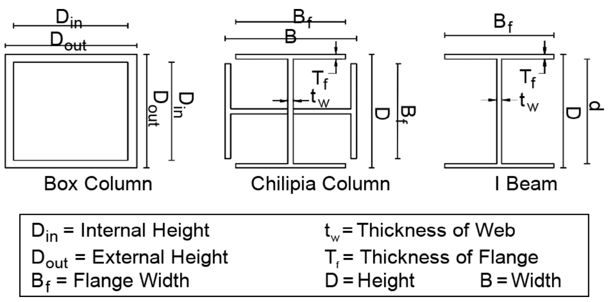

Figure 1. Beam and column sections.

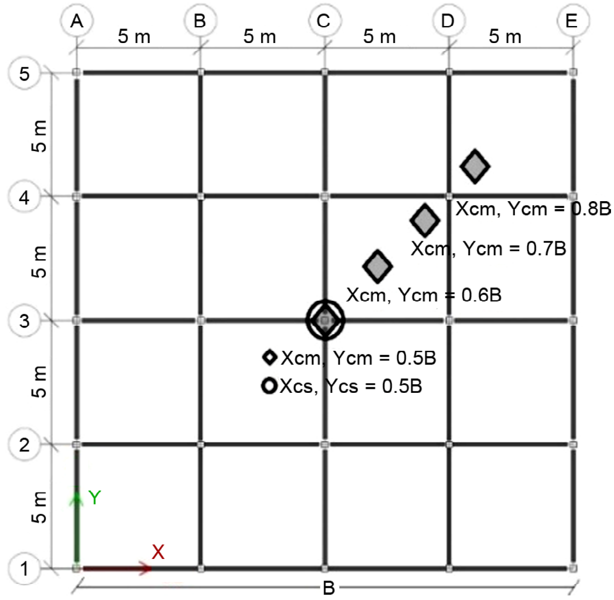

Figure 2. Modeling of irregularity by considering center of stiffness (CS) and center of mass (CM) at different locations in plan.

2.4. Loading Pattern

In this study, the structures are designed to withstand gravity and lateral loads; i.e., dead and

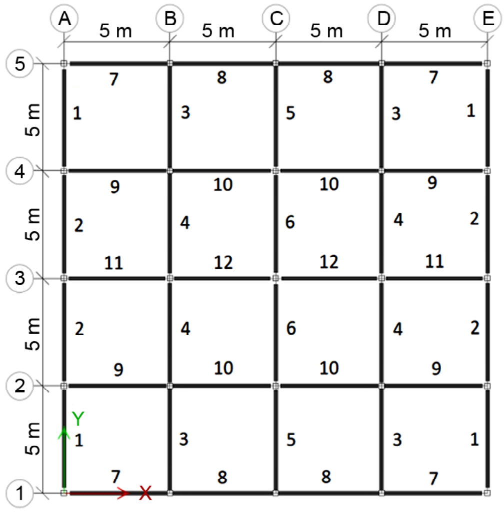

(a) Grouping of Beams

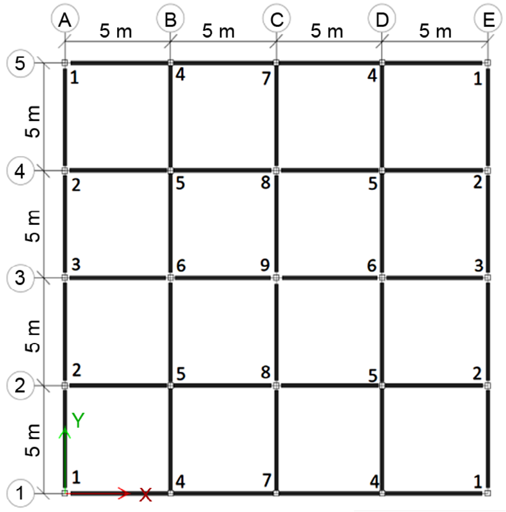

(b) Grouping of Columns

Figure 3. Symmetric member grouping in plan.

live loads and earthquake effects. Seismic demands were evaluated by equivalent static analysis method. The structural elements are to be designed for Equation (2) combination effect as per ASCE specifications:

$$1.2D + LL + Ex \qquad (2)$$

where *DL*, *LL*, *Ex* are dead load, live load and seismic load in X-direction, respectively. Earthquake load (*E*) is determined by equivalent static force method. The *E* value is calculated based on a coefficient (*Cs*) of effective seismic weight. *Cs* variable which is related to the acceleration of design (*A*), importance factor (*I*), response modification coefficient (*R*), site class and structure height is calculated according to 2800 code design [16].

2.5. Structural Analysis

For structural analysis, a set of finite element methods of OpenSEES software has been used. In structural analysis, the effects of P-Δ have also been applied.

2.6. Constraints

In fact, the constraint (*G*) in a structural optimization, is evaluation of a member or structure design response (q_i) with maximum allowable absolute value ($q_{allow,i}$), which is expressed as Equation (3):

$$G = |q_i| - q_{allow,i} \le 0 \qquad (3)$$

In this research, constraints are divided into three categories: design, seismic and geometric, which are according to AISC 3610-10 [18] and seismic constraints provisions of AISC code. The constraints details are expressed as follows:

2.6.1. Design Constraints

a) According to AISC360-10 [18], double symmetric sections should be examined for minor and major bending and compressive axial forces as the Equations (4) and (5) conditions must be satisfied:

$$\frac{P_u}{\varphi_a P_c} > 0.2 \rightarrow \quad \frac{P_u}{\varphi_a P_n} + \frac{8}{9}\left(\frac{M_{ux}}{\varphi_b M_{nx}} + \frac{M_{uy}}{\varphi_b M_{ny}}\right) - 1.0 \le 0 \qquad (4)$$

$$\frac{P_u}{\varphi_a P_c} < 0.2 \rightarrow \quad \frac{P_u}{2\varphi_a P_n} + \frac{8}{9}\left(\frac{M_{ux}}{\varphi_b M_{cx}} + \frac{M_{uy}}{\varphi_b M_{cy}}\right) - 1.0 \le 0 \qquad (5)$$

where indices, *n*, *u*, *x*, *y*, *a* and *b* indicate nominal capacity, ultimate load, local direction X, local Direction Y, axial and bending, respectively. Also, *P*, *M* and φ specify axial forces, bending moments and strength reduction factor, respectively.

b) The slenderness ratio (k_L/r) should be limited to 200 for the major local direction where *L*, *r* and k, denote element length, radius of gyration, and unbraced length ratio, respectively.

c) The width to thickness ratios of the compression elements must comply with the compact section criteria.

2.6.2. Seismic Constraints

a) Displacement and drift constraint: In this research, roof displacement and inter-story drift must satisfy Equations (6) and (7), respectively according to AISC360-10 specification [18]:

$$G_{s1} = \frac{\frac{\Delta_{roof}}{H}}{Dr_{allow}} - 1 \le 0 \tag{6}$$

$$G_{s2} = \frac{\Delta_{st} * C_d}{Q * h} - 1 \le 0 \tag{7}$$

where, Δ_{roof}, H and Dr_{allow} are roof displacement, structure height and allowable roof drift. Also Δ_{st}, C_d, Q and h, are story displacement, nonlinear displacement coefficient, allowable displacement and story height. All allowable values can be calculated according to AISC provision [18].

b) Weak beam strong column constraint: In this study, joints must satisfy weak beam-strong column constraint expressed as Equation (8):

$$G_{s3} = \frac{\sum M_{pci}}{\sum M_{pbi}} - 1 = \frac{\sum Z_c \left(F_y - \frac{P_{uc}}{A_g} \right)}{\sum 1.1 R_y F_y Z_b + M_{uv}} \le 0 \tag{8}$$

In equations described above, all variables can be obtained according to AISC 360-10 regulation [18].

2.6.3. Geometric Constraints

In joints, the geometric dimensions of the beams and columns as shown in Figure (4) must satisfy the ideal conditions as Equations (9) to (11):

$$G_{G1} = \frac{D_{outT,i}}{D_{outB,i}} - 1 \le 0 \tag{9}$$

$$G_{G2} = \frac{B_{fi}}{D_{outB,i}} - 1 \le 0 \tag{10}$$

$$i = 1, 2, 3, \ldots, N_{joint} \tag{11}$$

In the above relations, $D_{outT,i}$ and $D_{outB,i}$ are the outer dimensions of upper and lower columns

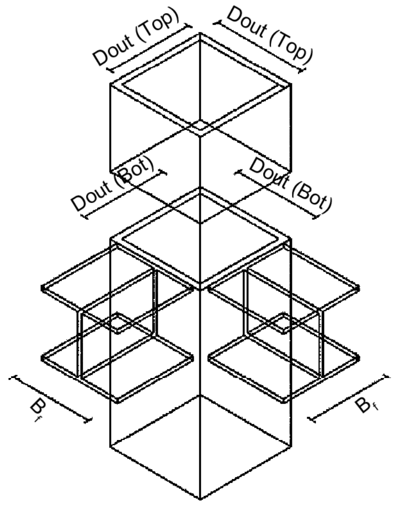

Figure 4. Overviews of connections.

in joint *i*, respectively. Also B_f is the width of the beam's flange in joint i.

2.7. Penalty Function

If any of the previously mentioned constrains are not satisfied, the objective function is penalized by Equation (12) relation. The penalty is based on the amount of violation of the corresponding constraint:

$$P = (1 + C)^{\varepsilon} \times W \tag{12}$$

where P, W and C are the penalized function, weight of the structure and the magnitude of the violation, respectively. A value of $\varepsilon = 1$ is taken for this study.

3. Particle Swarm Optimization Algorithm

Particle swarm optimization (PSO) is a population-based algorithm proposed by Kennedy and Eberhart [2], which was inspired by the social behavior of animals such as fishes schooling, birds flocking, and insects swarming. Similar to other population-based algorithms, many researchers try this method to solve optimum problems. Dogan and Saka [19] optimized unbraced steel frames by the mentioned algorithm while applying LRFD-AISC design constraint. Results show that the particle swarm optimizer achieve lighter frame weights compared to other meta-heuristic methods. Therefore, it can be concluded that PSO is an efficient and robust algorithm for optimal design of steel structures. In another field work, a discrete

PSO algorithm was employed for optimal design of 2D and 3D steel frames using Euro code 3 criteria for constraints. A comparison with discrete GA revealed that the PSO exhibited better convergence speed with smaller computational cost. This fact is due to the more complex and time-consuming procedures of GA as part of the genetic operators of the algorithm [20]. The PSO was also used for optimal design of composite and non-composite steel floor systems using the Canadian S16 design standard criteria as constraints to minimize the floor mass or its construction costs. In the process of minimizing the cost function, it was observed that the composite floors can be as economical as non-composite floors [21]. All the research above approves the ability of particle swarm algorithm. In this study, the algorithm was performed as follows:

In the PSO algorithm, a v-dimensional search space is defined based on the number of variables for the problem and within this space, a set of particles is randomly generated. Each random particle can be the answer of the problem under consideration. The quality of search space's particles is evaluated by the objective function defined for the problem. In the optimization process, these particles are constantly on the move to find the best possible answer. By experiencing more new places in the search space, better answers will be obtained with particles. By this process, the algorithm eventually converges to an appropriate answer that can be optimal or close to the final optimal solution. Two factors are effective in converging the algorithm's efforts to better answers, local best position (p_{best}) and global best position (g_{best}). In the search space, the best position experienced by the ith particle under study is called pbest, while gbest is called the best position experienced by all particles so far. Accordingly, the position of particles in society in each iteration is modified as Equations (13) and (14):

$$V_i^{(k+1)} = wv_i^{\,k} + c_1 r_1 \left(pbest_i^{\,k} - x_i^{\,k}\right) + c_2 r_2 \left(gbest_i^{\,k} - x_i^{\,k}\right) \tag{13}$$

$$x_i^{\,k+1} = x_i^{\,k} + v_i^{\,k+1} \tag{14}$$

where $v_i^{\,k}$ and $x_i^{\,k}$ are the velocity and the position of the i^{th} particle at the k^{th} iteration, respectively; r_1 and r_2 denote random numbers from domain [0, 1]. W is a function of linearly decreasing velocity according to Equation (15), which limits the range of particle velocity changes.

$$W = \frac{2*k}{\left|2-\varphi-\sqrt{\varphi*(\varphi-4)}\right|} \tag{15}$$

In W equation, φ is expressed as, sum of the C_1 and C_2 coefficients and is equal to 4.1 and the value of 2.05 is applied for C_1 and C_2.

PSO is briefly described in the following steps:

- Step 1: Initialization.

First, the variables of PSO algorithm are defined. The initial position of all particles then is randomly generated in the allowable domain. At last, the particles are evaluated by the objective function of the problem and pbesti and gbest are extracted and saved.

- Step 2: Updating procedure.

In this step positions and velocities of each particle are updated according to Equations (13) and (14). Then, the objective function is assessed using all the particles and the new pbesti and gbest are updated.

- Step 3: Terminating criterion.

Once a predefined stopping condition is fulfilled, the process is terminated. Otherwise, the step 2 is repeated. In this research, the termination criterion is a specific weight difference (0.001) between consecutive iterations for 50 iterations.

4. Examples

In this section, two examples were expressed. The box-shaped columns structure is first optimized with irregularities explained at section 2.3 and the outputs are compared. Then the cross-shaped columns structure is optimized and evaluated with the same condition as the first example. The shape of the beam and column sections in the two examples is depicted in Figure (1). MATLAB software was used to implement the optimization algorithm and design constraints. Additionally, OpenSEES software was used to analyze the example's structures. The results of the analysis associated with the OpenSEES and design constraints results in MATLAB have been validated with the outputs of ETABS software (2015). All the design, performance, and seismic criteria have been applied in according to Section 2.6. In this research, the steel's yield strength and modulus of elasticity are considered equal to $f_y = 240$ Mpa and $E = 200$ Gpa. Equivalent static analysis has been used to calculate the earthquake load. The soil class parameters, *A*, *R*, *I* and C_d used in the equivalent static analysis are equal to *C*, 0.25, 5, 1 and 4, respectively. Also the value of *B* is considered 2.75 (calculated from 2800 code design [16]).

In examples, PSO algorithm is employed to optimize the models. The parameters of mentioned algorithm are applied as follows:

- The number of iterations (*k*) considered: 400.
- The number of initial populations considered: 100.
- The value 2.05 is applied for C_1 and C_2.

4.1. Example 1

In this example, a three-story three-dimensional moment frame is considered as shown in Figure (5). This frame has four 5-m spans in the x and y direction. The height of the story is 3.2 m. Gravity loads including dead load and live load on the floors are 4.5 kN/m^2 and 2.0 kN/m^2 and on the roof are 4.5 kN/m^2 and 1.5 kN/m^2, respectively. Also, for floor's walls, uniform distributed dead loads are assigned with the beams around the structure as 7.56 kN/m, and for walls of the roof are assigned as 2.45 kN/m. The column sections in structure are considered HSS-shaped and the sections of the beams are applied W-shaped. Columns and beams, divided into 27 and 32 groups respectively, as shown in Figure (3). The structure at least is modeled with 0, 20, 40 and 60 percent eccentricity to consider irregularities as expressed in section 2.4. Then the outputs were compared. The comparative results are presented in Table (1). The comparison of the obtained sections is shown in Table (2). The optimization history and best optimum cost results are expressed in Figures (6)

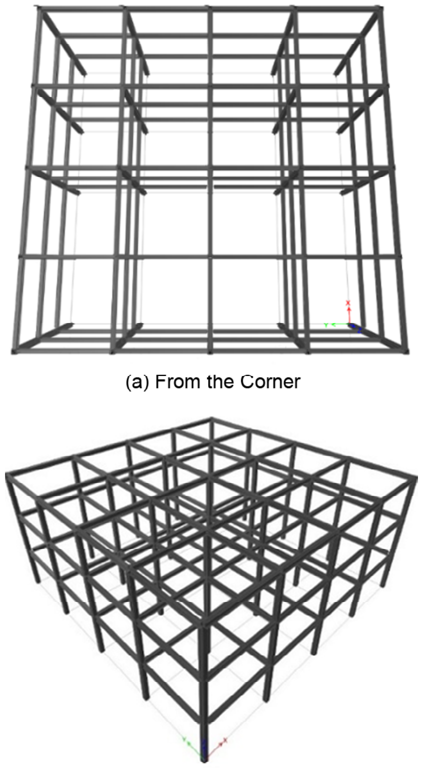

(a) From the Corner

(b) From the Top

Figure 5. Different views of the structure.

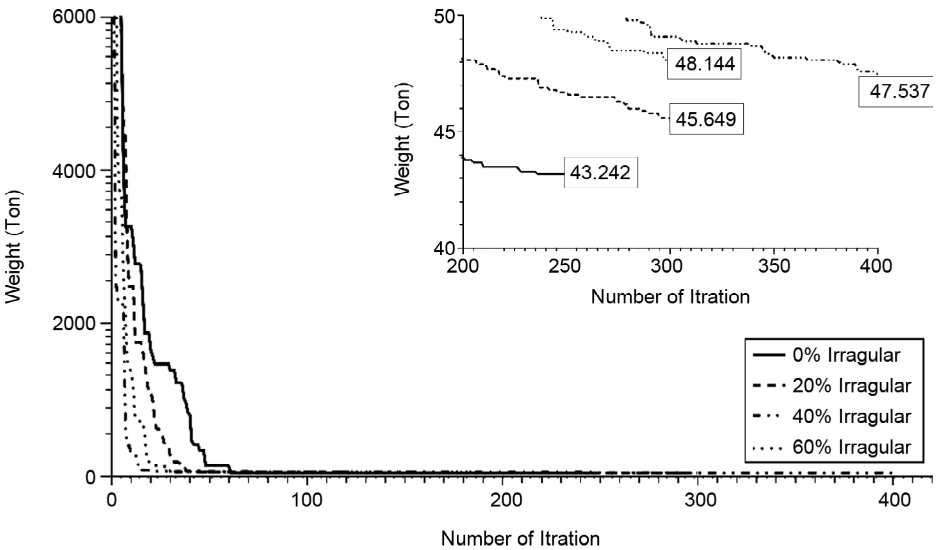

Figure 6. Convergence histories of the 3-story structures (Example 1).

and (7). Also, the roof displacement, strength and inter-story drift ratio are shown in Figures (8) to (10), respectively.

4.2. Example 2

A 3-story 3D moment frame shown in Figure (5) is considered as the second example. The length

Table 1. Comparative results of the considered algorithm for the 3-story structure with W beams and HSS columns (Example 1).

Algorithm	Runs	Regular		%20 Irregular		%40 Irregular		%60 Irregular	
		Weight (ton)	Weight Ratio*	Weight (ton)	Weight Ratio*	Weight (ton)	Weight Ratio*	Weight (ton)	Weight Ratio*
Pso	4000	**43.242**	**1.00**	45.649	1.055	47.537	1.099	48.144	1.113

* "Weight ratio" is the comparison ratio between regular and irregular structures * The bold number is the smallest result

Table 2. Comparative system results of the 3-story structures (Example 1).

Group	Regular		%20 Irregular		%40 Irregular		%60 Irregular	
	Beams	Columns	Beams	Columns	Beams	Columns	Beams	Columns
1	W12X19	HSS8X8X1/2	W12X22	HSS10X10X1/2	W12X19	HSS10X10X1/2	W14X22	HSS10X10X1/2
2	W12X19	HSS14X14X5/8	W14X34	HSS16X16X6/8	W16X31	HSS12X12X1/2	W12X22	HSS12X12X1/2
3	W12X14	HSS10X10X1/2	W16X26	HSS16X16X1	W12X16	HSS12X12X5/8	W12X19	HSS16X16X1
4	W12X16	HSS10X10X1/2	W12X14	HSS14X14X5/8	W12X19	HSS12X12X1/2	W12X14	HSS12X12X1/2
5	W12X16	HSS16X16X1	W14X34	HSS12X12X1/2	W12X22	HSS14X14X5/8	W16X31	HSS14X14X5/8
6	W12X14	HSS14X14X5/8	W12X16	HSS14X14X5/8	W12X19	HSS16X16X6/8	W12X22	HSS14X14X5/8
7	W14X22	HSS10X10X5/8	W12X22	HSS12X12X1/2	W18X35	HSS12X12X1/2	W14X22	HSS12X12X1/2
8	W12X19	HSS12X12X1/2	W12X22	HSS12X12X1/2	W14X30	HSS12X12X5/8	W16X26	HSS16X16X1
9	W16X26	HSS12X12X1/2	W12X19	HSS14X14X5/8	W12X26	HSS14X14X5/8	W18X40	HSS12X12X1/2
10	W14X22	HSS8X8X1/2	W12X22	HSS10X10X1/2	W18X35	HSS10X10X5/8	W18X40	HSS10X10X1/2
11	W14X22	HSS14X14X5/8	W14X22	HSS12X12X1/2	W16X31	HSS10X10X1/2	W16X26	HSS12X12X1/2
12	W14X22	HSS10X10X1/2	W12X22	HSS16X16X6/8	W12X16	HSS12X12X5/8	W14X22	HSS10X10X5/8
13	W12X19	HSS10X10X1/2	W14X22	HSS14X14X5/8	W14X22	HSS12X12X5/8	W18X35	HSS10X10X1/2
14	W12X19	HSS14X14X5/8	W14X22	HSS12X12X1/2	W12X19	HSS14X14X6/8	W12X19	HSS14X14X5/8
15	W12X14	HSS14X14X6/8	W12X14	HSS14X14X5/8	W18X35	HSS14X14X5/8	W12X14	HSS14X14X5/8
16	W12X14	HSS10X10X5/8	W12X16	HSS12X12X1/2	W16X31	HSS12X12X5/8	W12X16	HSS12X12X5/8
17	W14X30	HSS12X12X5/8	W12X16	HSS10X10X1/2	W16X31	HSS12X12X5/8	W14X22	HSS12X12X1/2
18	W12X26	HSS12X12X5/8	W12X16	HSS12X12X1/2	W16X26	HSS12X12X5/8	W12X26	HSS10X10X1/2
19	W16X31	HSS8X8X5/8	W14X22	HSS6X6X3/8	W14X22	HSS6X6X3/8	W12X22	HSS8X8X5/8
20	W12X19	HSS10X10X1/2	W12X22	HSS6X6X3/8	W14X22	HSS10X10X1/2	W14X30	HSS12X12X1/2
21	W16X26	HSS10X10X1/2	W12X26	HSS10X10X1/2	W18X40	HSS6X6X5/16	W12X22	HSS8X8X5/8
22	W12X19	HSS10X10X1/2	W14X22	HSS10X10X1/2	W14X34	HSS10X10X1/2	W14X22	HSS10X10X5/8
23	W14X22	HSS10X10X1/2	W12X22	HSS8X8X1/2	W18X40	HSS8X8X1/2	W12X19	HSS6X6X1/2
24	W16X31	HSS10X10X1/2	W16X31	HSS6X6X1/4	W12X16	HSS10X10X1/2	W12X26	HSS10X10X5/8
25	W14X22	HSS6X6X5/16	W18X35	HSS10X10X1/2	W12X19	HSS10X10X1/2	W12X19	HSS8X8X1/2
26	W14X30	HSS8X8X1/2	W12X19	HSS10X10X5/8	W18X35	HSS10X10X5/8	W14X22	HSS10X10X1/2
27	W12X16	HSS10X10X5/8	W12X19	HSS12X12X1/2	W12X19	HSS8X8X5/8	W12X14	HSS10X10X5/8
28	W12X16		W12X14		W12X14		W12X22	
29	W12X16		W16X31		W16X26		W12X14	
30	W12X14		W12X14		W18X40		W30X90	
31	W18X35		W12X22		W16X26		W12X19	
32	W12X19		W12X19		W14X22		W18X35	
33	W16X26		W12X19		W18X35		W14X22	
34	W21X44		W30X90		W12X22		W12X19	
35	W12X22		W12X22		W12X26		W14X34	
36	W12X16		W12X19		W16X31		W14X22	
W(ton)	**43.242**		45.649		47.537		48.144	
W(ratio)	**1**		1.055		1.099		1.113	

of spans is 5 m, and the height of the stories is 3.2 m. Gravity and lateral loads on the structure are the same as in the previous example. The columns and beams are assigned cross-shaped and W-shaped sections, respectively. Columns are arranged in 27 groups and beams are divided into 32 groups, as shown in Figure (3). The structure is modeled in same eccentricity condition as the previous example and then the results were compared. The comparative results are presented

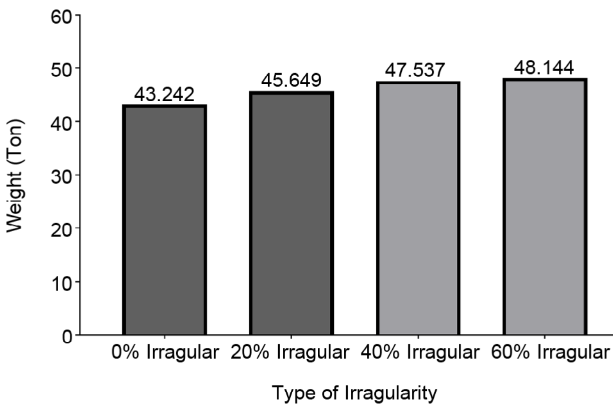

Figure 7. Best optimum cost results of the 3-story structures (Example 1).

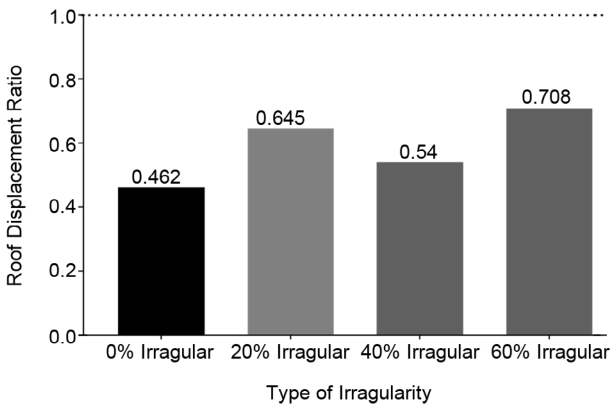

Figure 8. Roof Displacement ratios of optimum results of the 3-story structures (Example 1).

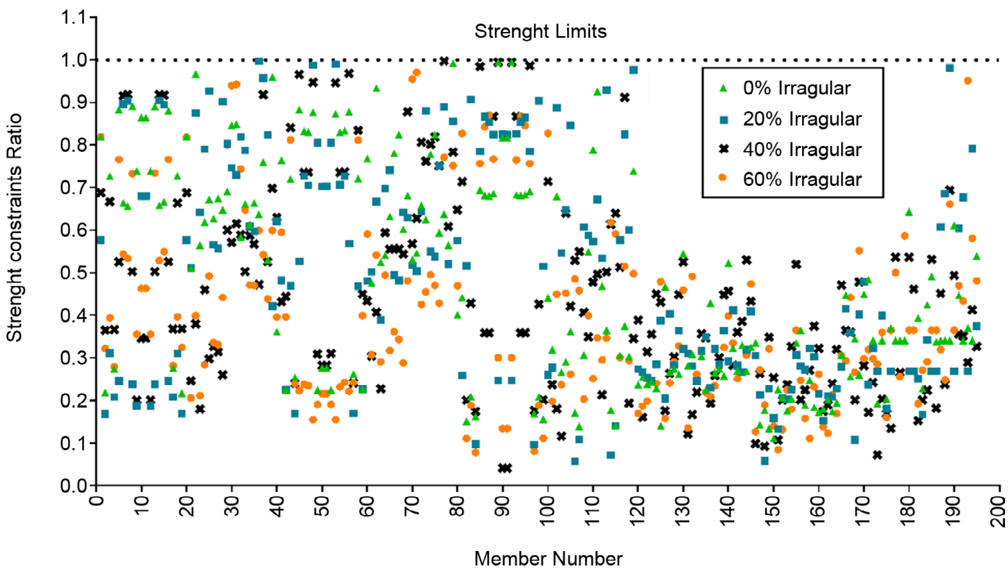

Figure 9. Strength ratios of members of optimum results of the 3-story structures (Example 1).

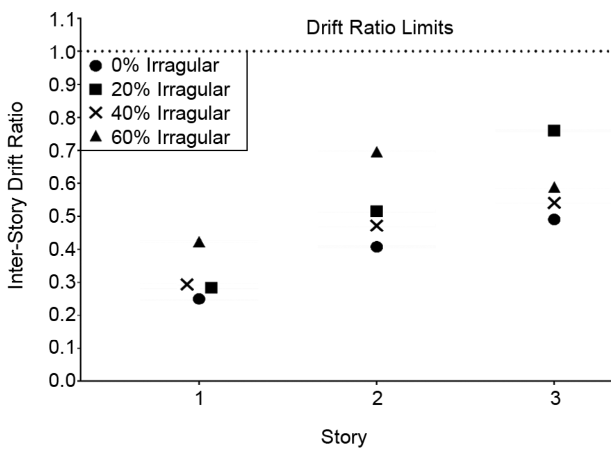

Figure 10. Inter-story drift ratios of optimum results of the 3-story structures (Example 1).

in Table (3). The comparison of the obtained sections is shown in Table (4). The optimization history and best optimum cost results are expressed in Figures (11) and (12). Also, the roof displacement, strength and inter-story drift ratio are shown in Figures (13) to (15), respectively.

Table 3. Comparative results of the considered algorithm for the 3-story structure with w-shaped beams and cross-shaped columns (Example 2).

Algorithm	Runs	Regular		%20 Irregular		%40 Irregular		%60 Irregular	
		Weight (ton)	Weight Ratio*	Weight (ton)	Weight Ratio*	Weight (ton)	Weight Ratio*	Weight (ton)	Weight Ratio*
Pso	4000	**54.915**	**1.00**	55.114	1.003	6.009	1.094	61.465	1.119

* "Weight ratio" is the comparison ratio between regular and irregular structures * The bold number is the smallest res

Table 4. Comparative system results of the 3-story structure (Example 2).

Group	Regular		%20 Irregular		%40 Irregular		%60 Irregular	
	Beams	Columns	Beams	Columns	Beams	Columns	Beams	Columns
1	W12X22	Cross_2w24x68	W12X22	Cross_2w21x44	W12X19	Cross_2w21x50	W12X19	Cross_2w18x35
2	W16X31	Cross_2w21x50	W16X31	Cross_2w21x50	W14X30	Cross_2w24x68	W12X16	Cross_2w24x68
3	W18X40	Cross_2w24x55	W16X26	Cross_2w24x76	W21X50	Cross_2w24x68	W12X19	Cross_2w30x108
4	W12X22	Cross_2w18x35	W12X16	Cross_2w24x68	W12X19	Cross_2w24x84	W10X12	Cross_2w24x55
5	W16X31	Cross_2w24x76	W18X35	Cross_2w24x76	W24X55	Cross_2w24x76	W24X76	Cross_2w21x62
6	W16X31	Cross_2w24x55	W12X16	Cross_2w24x68	W10X12	Cross_2w27x84	W18X40	Cross_2w33x130
7	W12X22	Cross_2w21x68	W16X31	Cross_2w30x108	W18X35	Cross_2w30x108	W12X22	Cross_2w27x84
8	W16X26	Cross_2w30x90	W18X35	Cross_2w30x90	W18X35	Cross_2w24x76	W16X31	Cross_2w33x118
9	W12X26	Cross_2w40x167	W12X16	Cross_2w33x118	W14X22	Cross_2w40x167	W18X35	Cross_2w36x135
10	W18X40	Cross_2w24x55	W14X34	Cross_2w21x44	W12X16	Cross_2w21x44	W12X16	Cross_2w18x35
11	W12X16	Cross_2w18x40	W12X14	Cross_2w21x50	W12X26	Cross_2w18x35	W12X14	Cross_2w18x40
12	W10X12	Cross_2w18x40	W14X22	Cross_2w24x55	W10X12	Cross_2w21x44	W10X12	Cross_2w18x40
13	W14X22	Cross_2w18x35	W14X22	Cross_2w21x50	W12X22	Cross_2w24x55	W14X30	Cross_2w21x50
14	W14X22	Cross_2w24x68	W12X22	Cross_2w24x68	W14X22	Cross_2w21x68	W12X22	Cross_2w18x35
15	W12X22	Cross_2w24x55	W12X16	Cross_2w21x50	W18X40	Cross_w21x50	W12X26	Cross_2w30x99
16	W14X30	Cross_2w16x31	W12X14	Cross_2w18x35	W12X14	Cross_2w30x90	W14X22	Cross_2w21x68
17	W12X22	Cross_2w24x68	W14X22	Cross_2w24x55	W14X22	Cross_2w14x34	W24X68	Cross_2w30x99
18	W18X40	Cross_2w30x116	W18X35	Cross_2w30x90	W12X26	Cross_2w30x99	W14X30	Cross_2w30x116
19	W12X22	Cross_2w14x30	W18X35	Cross_2w14x34	W12X22	Cross_2w16x31	W18X35	Cross_2w14x34
20	W12X19	Cross_2w14x22	W12X19	Cross_2w14x34	W16X26	Cross_2w12x22	W16X26	Cross_2w16x31
21	W14X30	Cross_2w16x26	W21X44	Cross_2w16x26	W12X19	Cross_2w16x26	W16X26	Cross_2w12x22
22	W14X22	Cross_2w14x22	W14X22	Cross_2w14x22	W14X22	Cross_2w12x22	W14X22	Cross_2w14x30
23	W12X22	Cross_2w16x31	W18X35	Cross_2w12x16	W16X26	Cross_2w18x35	W14X30	Cross_2w18x35
24	W12X16	Cross_2w21x50	W12X26	Cross_2w16x26	W12X22	Cross_2w16x26	W24X55	Cross_2w24x68
25	W16X31	Cross_2w14x22	W14X22	Cross_2w12x19	W14X22	Cross_2w12x26	W18X40	Cross_2w30x108
26	W12X19	Cross_2w18x35	W12X26	Cross_2w14x22	W14X34	Cross_2w14x30	W14X22	Cross_2w24x55
27	W12X14	Cross_2w14x30	W12X16	Cross_2w12x26	W12X22	Cross_2w27x84	W14X22	Cross_2w21x62
28	W12X14		W12X14		W12X14		W12X22	
29	W30X90		W14X34		W18X35		W14X34	
30	W12X16		W16X26		W12X14		W14X22	
31	W12X19		W12X16		W12X22		W12X16	
32	W14X22		W16X31		W21X44		W24X55	
33	W16X31		W14X34		W21X50		W21X44	
34	W12X22		W12X14		W12X16		W12X16	
35	W12X16		W14X34		W21X62		W12X16	
36	W14X22		W12X14		W16X26		W12X16	
W(ton)	**54.915**		55.114		60.009		61.465	
W(ratio)	**1**		1.003		1.094		1.119	

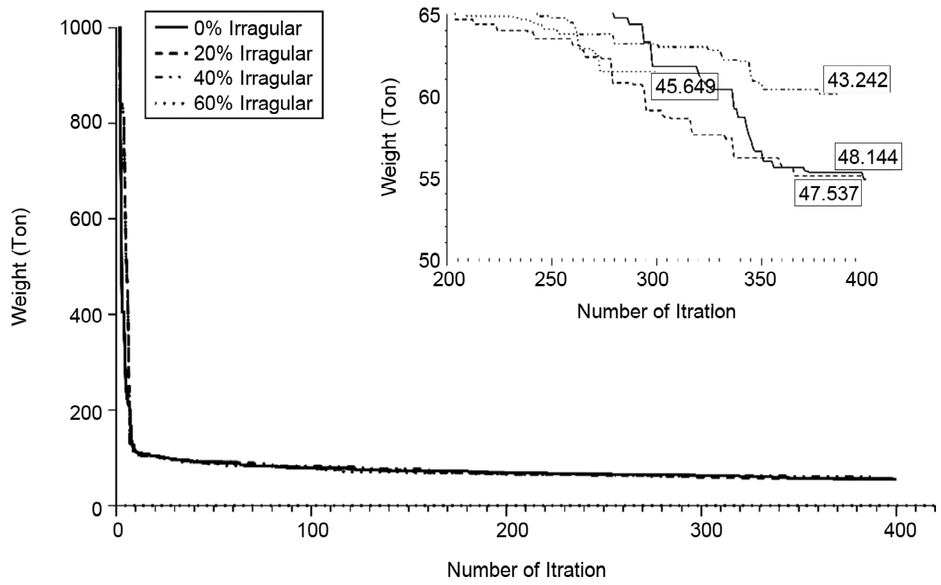

Figure 11. Convergence histories of the 3-story structures (Example 2).

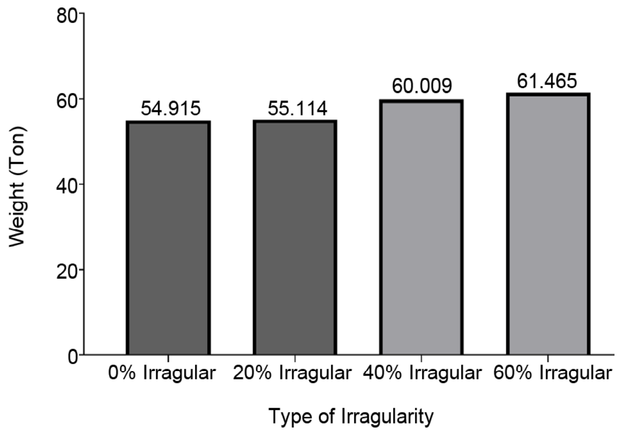

Figure 12. Best optimum cost results of the 3-story structures (Example 2).

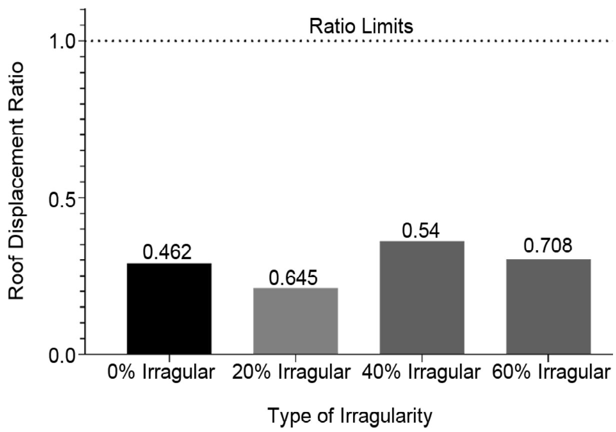

Figure 13. Roof displacement ratios of optimum results of the 3-story structures (Example 2).

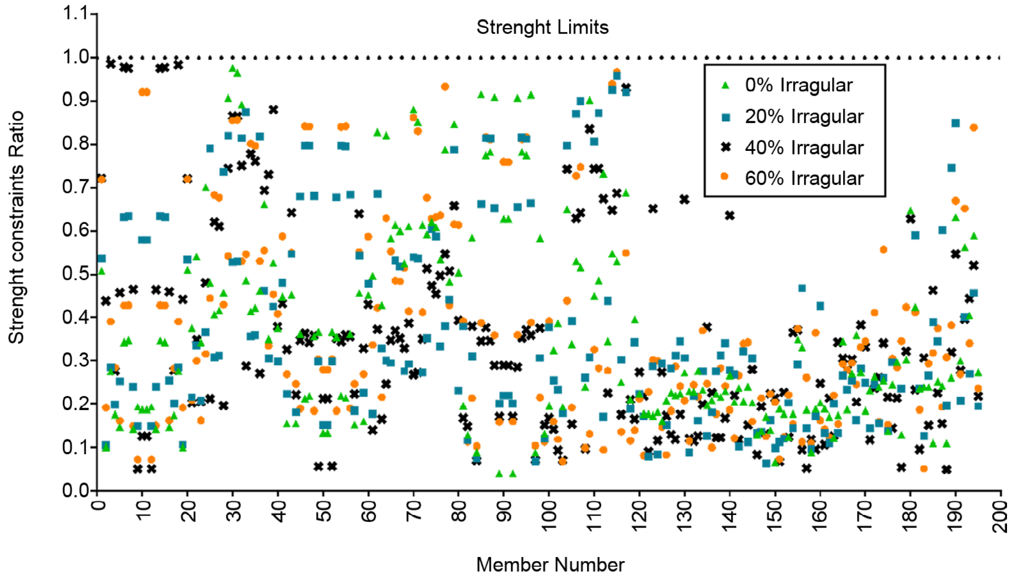

Figure 14. Strength ratios of members in optimum results of the 3-story structures (Example 2).

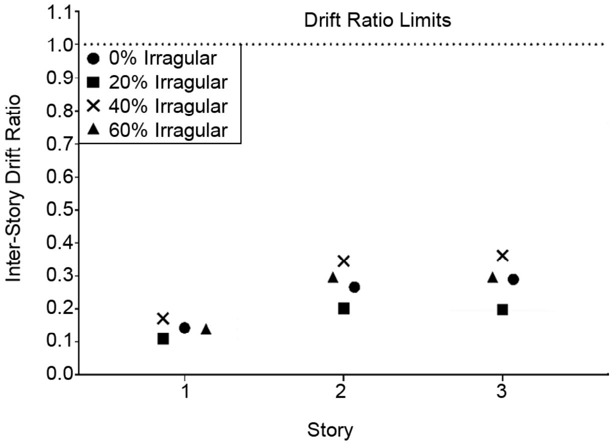

Figure 15. Inter-story drift ratios of optimum results of the 3-story structures (Example 2).

5. Conclusion

In this research, regular and irregular 3D moment frame structures with box and cross-shaped columns were optimized. The aim of this study (in optimization process) was evaluating the effect of various irregularities on optimum weight of structures. Also, the comparison between optimal weight of box and cross-shaped column models in different ratios irregularity was investigated. The method used in optimization process was PSO algorithm. Also, design, seismic and geometric criteria were considered. For implementation of the criteria mentioned, MATLAB software was used. OpenSEES software also was implemented for modeling and analyzing structures.

In the first example, the regular box-shaped column structure's weight was 43.242 tons, which was the lowest weight compared to the irregular models. Structures with 20, 40 and 60 percent load eccentricity had 5.5, 9.9 and 11.3 percent more weights than regular one. The results represented that despite high values of eccentricity, the algorithm managed to provide designs with less than 12 percent weight increase, while it has been proven that irregularities and torsion have a large effect on the weight of the structure. Therefore, by using the proposed algorithm designers can design lighter and economical structures.

In the second example, structure with cross-shaped columns in the regular state weighed 54.915 ton that was the best result. Also, the 20, 40 and 60 percent eccentric models were 0.3, 9.4 and 11.3 percent weighted more than the best one (regular model).

From the comparative results of the two examples, it can be concluded that structures with HSS columns had better optimal weight than structures with cross-shaped columns. It shows using box-shaped column is better than cross-shaped columns in the same conditions. Also, it can be obtained that choosing correct sections can have a great impact on the optimum weight of a structure. Also, it can be observed that the rate of weight changing by considering different irregularity is almost constant in optimized structures with different sections. For instance, for each %20 increase of eccentricity, the weight of the optimal structure will increase by about %5.

This research can be expanded to investigate the effect of analysis types on the optimum weight. Furthermore, the influence of grouping elements on the structure optimized weight can be assets.

6. Declarations

Funding: No funds, grants, or other support was received.

Conflict of interest: The authors have no relevant financial or non-financial interests to disclose.

Code availability: On behalf of all authors, the corresponding author states that the results presented in this paper can be reproduced by the implementation details provided herein. The datasets generated during the current study are available from the corresponding author on reasonable request.

References

1. Goldberg, D.E. and Holland, J.H. (1988) *Genetic Algorithms and Machine Learning.*

2. Eberhart, R. and Kennedy, J. (1995) A new optimizer using particle swarm theoryþ. *Proceedings of the Sixth International Symposium on Micro Machine and Human Science*, Nagoya, Japan, 39-43.

3. Dorigo, M. and Maniezzo, V. (1996) Ant system: optimization by a colony of cooperating agents. *IEEE Transactions on Systems, Man, and Cybernetics, Part B* (Cybernetics), **26**(1),

29-41.

4. Geem, Z.W., Kim, J.H., and Loganathan, G.V. (2001) A new heuristic optimization algorithm: harmony search. *Simulation*, **76**(2), 60-68, doi:10.1177/003754970107600201.

5. Eslami, M., Shareef, H., Khajehzadeh, M., and Mohamed, A. (2012) A survey of the state of the art in particle swarm optimization. *Research Journal of Applied Sciences, Engineering and Technology*, **4**, 1181-1197.

6. Talatahari, S., Gandomi, A., Yang, X.-S., and Deb, S. (2015) Optimum design of frame structures using the eagle strategy with differential evolution. *Engineering Structures*, **91**, 10.1016/j.engstruct.2015.02.026.

7. Kaveh, A. and Talatahari, S. (2010) A discrete big bang-big Crunch algorithm for optimal design of skeletal structures. **11**(1), 103-122, Accessed: Aug. 17, 2021. [Online]. Available: https://www.sid.ir/en/Journal/ViewPaper.aspx?ID=185452.

8. Kaveh, A. and Talatahari, S. (2010) An improved ant colony optimization for the design of planar steel frames. *Engineering Structures*, **32**(3), 864-873.

9. Kaveh, A. and Talatahari, S. (2010) Optimum design of skeletal structures using imperialist competitive algorithm. *Computers and Structures*, **88**, 1220-1229, doi: 10.1016/j.compstruc.2010.06.011.

10. Aydogdu, I., Akin, A., and Saka, M.P. (2016) Design optimization of real world steel space frames using artificial bee colony algorithm with Levy flight distribution. *Advances in Engineering Software*, **92**, 1-14, doi: 10.1016/j.advengsoft.2015.10.013.

11. Murren, P. and Khandelwal K. (2014) Design-driven harmony search (DDHS) in steel frame optimization. *Engineering Structures*, **59**, 798-808.

12. Carbas, S. (2016) Design optimization of steel frames using an enhanced firefly algorithm. *Engineering Optimization*, **48**(12), 2007-2025, doi: 10.1080/0305215X.2016.1145217.

13. Aydogdu, I. and Saka, M.P. (2012) Ant colony optimization of irregular steel frames including elemental warping effect. *Advances in Engineering Software*, **44**(1), 150-169.

14. Eshaghi, M.S., Shishegaran, A., and Rabczuk, T. (2020) Evaluation of a novel ssymmetric genetic algorithm to optimize the structural design of 3D regular and irregular steel frames. *Frontiers of Structural and Civil Engineering*, **14**(5), 1110-1130, doi: 10.1007/S11709-020-0643-2.

15. Kaveh, A. and Ilchi Ghazaan, M. (2018) Optimum seismic design of 3D irregular steel frames using recently developed metaheuristic algorithms. *Journal of Computing in Civil Engineering*, **32**(3), p. 04018015, doi: 10.1061/(ASCE)CP.1943-5487.0000760.

16. BHRC Committee (2014) *Regulation for Designing Structures against Earthquake (2800 standard)*, 4th Ed., Iran, Tehran: Ministry of Housing and Urban Development.

17. Zheng, N., Yang, Z., Shi, C., and Chang, Z. (2004) Analysis of criterion for torsional irregularity of seismic structures. *13th World Conference on Earthquake Engineering Vancouver*, B.C., Canada, Paper No. 1465.

18. AISC Committee (2010) *Specification for Structural Steel Buildings (ANSI/AISC 360-10)*. Chicago-Illinois: American Institute of Steel Construction.

19. Dogan, E. and Saka, M.P. (2012) Optimum design of unbraced steel frames to LRFD-AISC using particle swarm optimizationþ. *Advances in Engineering Software*, **46**(1), 27-34.

20. Plevris, V., Batavanis, A.G., and Papadrakakis, M. (2011) Optimum design of steel structures with the particle swarm optimization method based on EC3. Available: http://www.vplevris.net/pdf_files/publications/C_22.pdf.

21. Poitras, G., Lefrançois, G. and Cormier, G. (2011) Optimization of steel floor systems using particle swarm optimization. *Journal of Constructional Steel Research*, **67**(8), 1225-1231.